Universidad de Guanajuato
División de Ciencias e Ingenierías

Spin-One Dark Matter and Gamma Ray Signals from the Galactic Center

XXXV Annual Meeting of the Division of Particles and Fields of the Mexican Physical Society

Haydee Hernández Arellano

Co-authors:
Dr. Mauro Napsuciale Mendívil
Dr. Simón Rodríguez Rodríguez

11 de mayo de 2021

Introduction

The elusive nature of dark matter

Dark matter (DM) contributes dominantly to the average energy density in the universe.

Its particle physics description remains **unknown**.

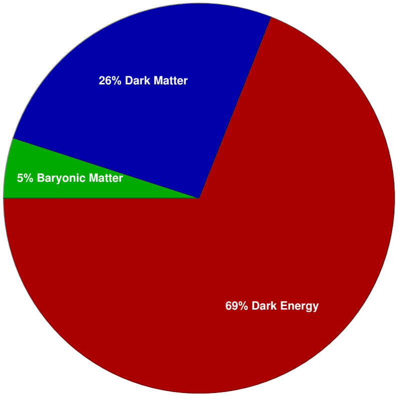

In order to discriminate between dark matter candidates, we have to check their consistency with

- Observations on astrophysical and cosmological scales, such as **relic density** ($\Omega_D h^2 = 0.120 \pm 0.001$ (Planck 2018)).
- Laboratory upper bounds on observables involving DM processes, such as **direct and indirect detection** limits.

Spin-One Dark Matter

Standard Model and extensions:

- Scalar Higgs $(0,0)$
- Quarks and leptons $(0,1/2)\oplus(1/2,0)$
- Gauge fields $(1/2,1/2)$
- Gravitino $(1,1/2)\oplus(1/2,1)$
- Graviton $(1,1)$

Our proposal

- $(1,0)\oplus(0,1)$ space-time structure for dark matter.
- Fields described by a six-component spinor.
- Kinetic term is not chiral.

M. Napsuciale, S. Rodríguez, R. Ferro-Hernández and S. Gómez-Ávila,
Phys. Rev. D93, 076003 (2016).
arXiv: 1509.07938

H. Hernández-Arellano, M. Napsuciale, and S. Rodríguez,
Phys. Rev. D98, 015001 (2018).
arXiv: 1801.09853

Spin-One DM interactions with SM

Considering the gauge group as $U(1)_D$:

$$\mathcal{L}_{int} = \bar{\psi}(g_s 1 + i g_p \chi)\psi\tilde{\phi}\phi + g_t\bar{\psi}M_{\mu\nu}\psi B^{\mu\nu} + \mathcal{L}_{\text{self-int}} \tag{1}$$

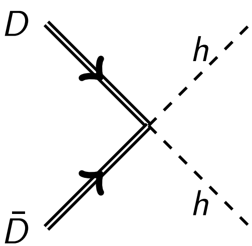

$$= i(g_s + i g_p \chi)$$

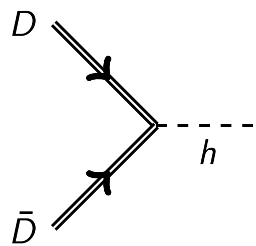

$$= i(g_s + i g_p \chi)v$$

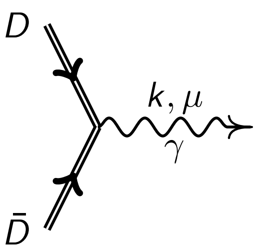

$$= 2g_t \cos\theta_W M^{\mu\nu} k_\nu$$

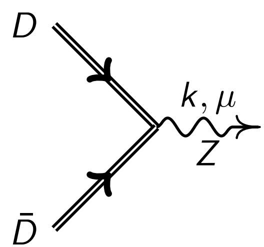

$$= -2g_t \sin\theta_W M^{\mu\nu} k_\nu$$

XENON1T limits

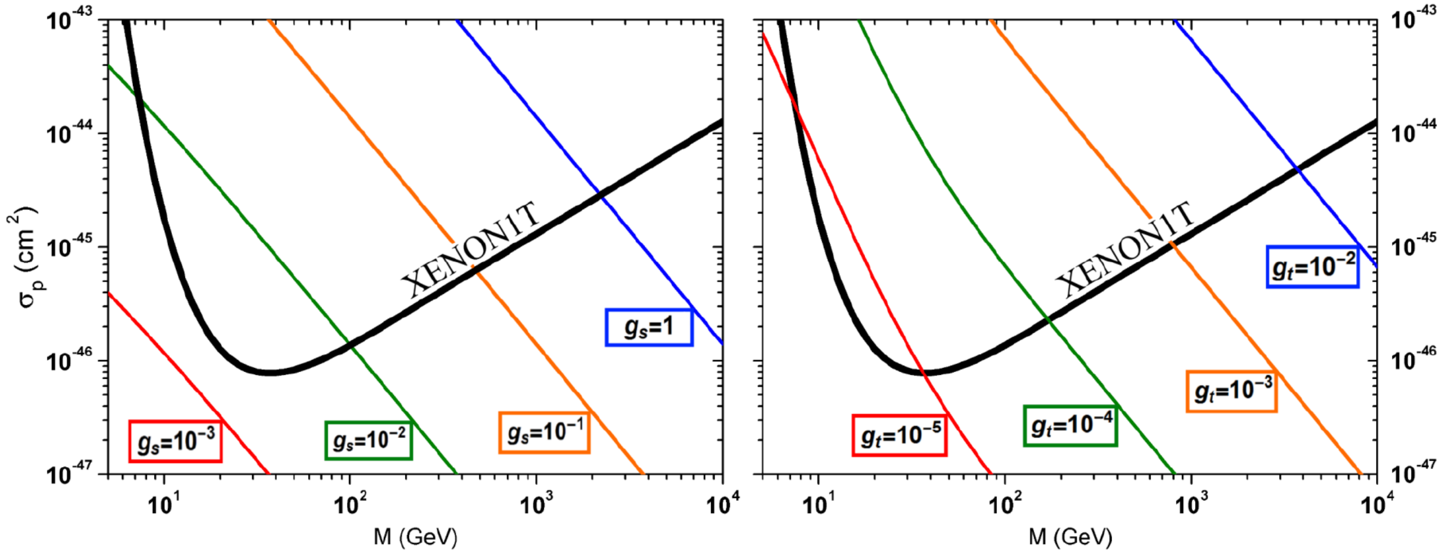

H. Hernández-Arellano, M. Napsuciale, and S. Rodríguez,
Phys. Rev. D98, 015001 (2018).
arXiv: 1801.09853

Gamma-Ray Excess in our Galactic Center

An excess in the gamma-ray flux from our Galactic Center has been claimed by several groups, centered around 3 GeV.

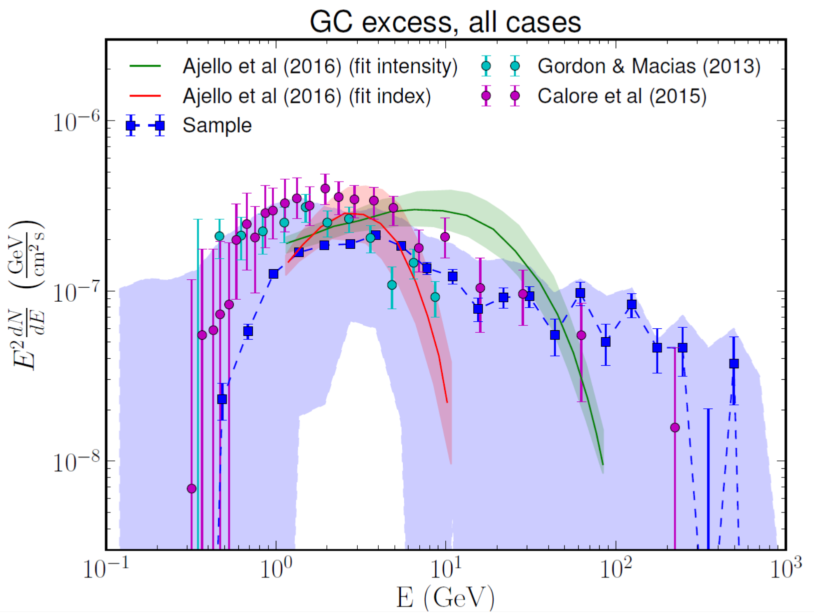

FermiLAT analysis: M. Ackermann et al., Astrophys. J. 840, 43 (2017).

Gamma-ray Differential Intensity

The GRE can be explained by some little known astrophysical sources, but **dark matter annihilation with photons in the final state** remains as an attractive possibility. Morphology of the emission consistent with this hipotesis.

- $\bar{D}D \to X\gamma$, with $X = H, Z^0$
- $\bar{D}D \to \gamma\gamma$
- $\bar{D}D \to R\gamma \to \bar{f}f\gamma$, with $R = \gamma, H, Z^0, \bar{Q}Q[^{2S+1}L_J]$

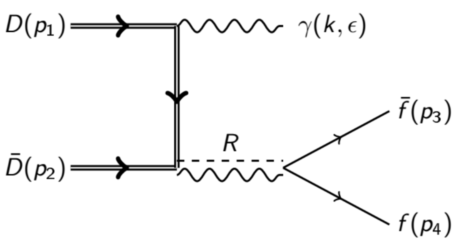

The gamma-ray differential flux from annihilation of (not-self-conjugated) dark matter is

$$\frac{d\Phi}{d\omega} = \sum_i \frac{1}{4} \frac{B_i}{4\pi M^2} \frac{d\langle \sigma v_r \rangle_i}{d\omega} \left(\int_{\Delta\Omega} \int_{l.o.s} \rho^2(\vec{l}) dl d\Omega \right) \qquad (2)$$

$\bar{D}D \to \bar{f}f$ cross section

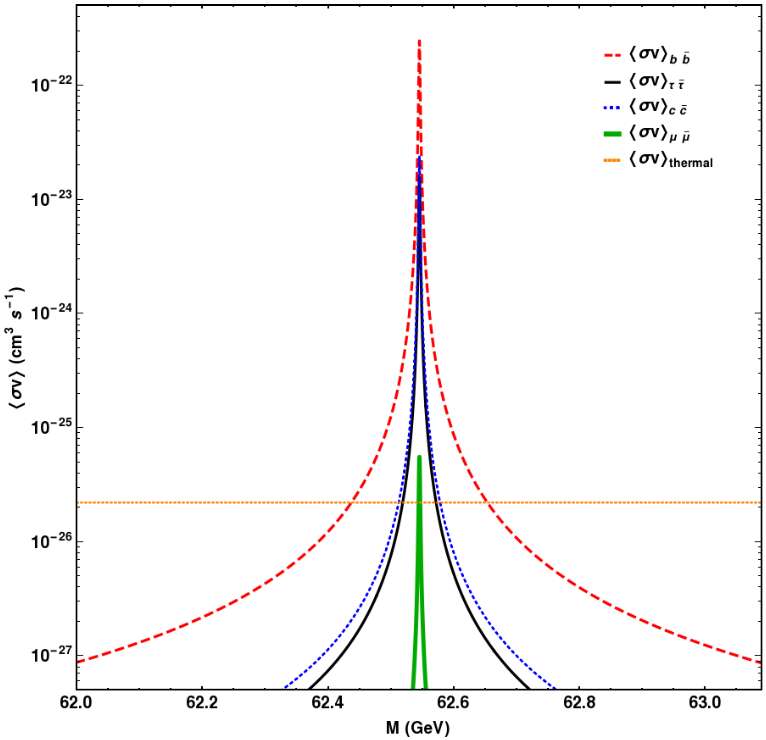

GRE can be explained through $\bar{D}D \to \bar{f}f$, for $M \in [5, 174]$ GeV, with $\langle \sigma v_r \rangle \approx 10^{-26} cm^3/seg \equiv \langle \sigma v_r \rangle_{\text{thermal}}$.

F. Calore, I. Cholis, C. McCabe and C. Weniger, Phys. Rev. D91, 063003 (2016).
arXiv: 1411.4647

$$M \approx M_H/2$$

GRE contributions from SODM

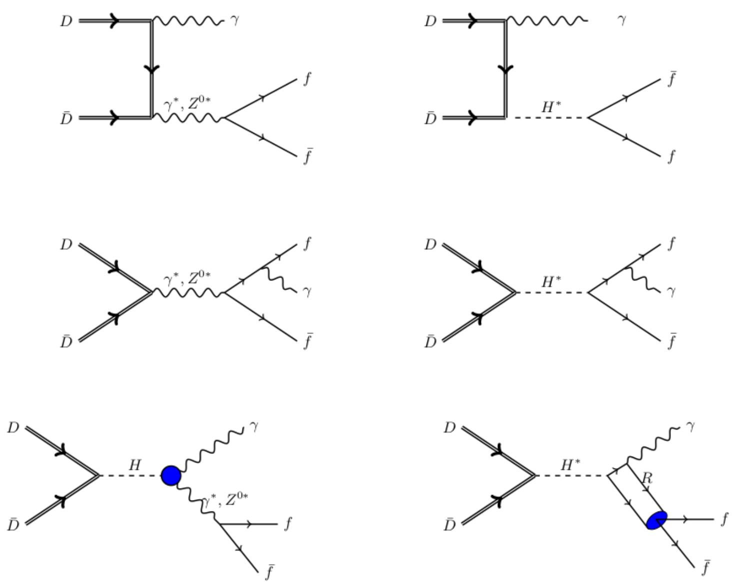

$\longleftarrow$ Initial state radiation.

$\longleftarrow$ Final state radiation.

$\longleftarrow$ Internal radiation.

GRE contributions from SODM

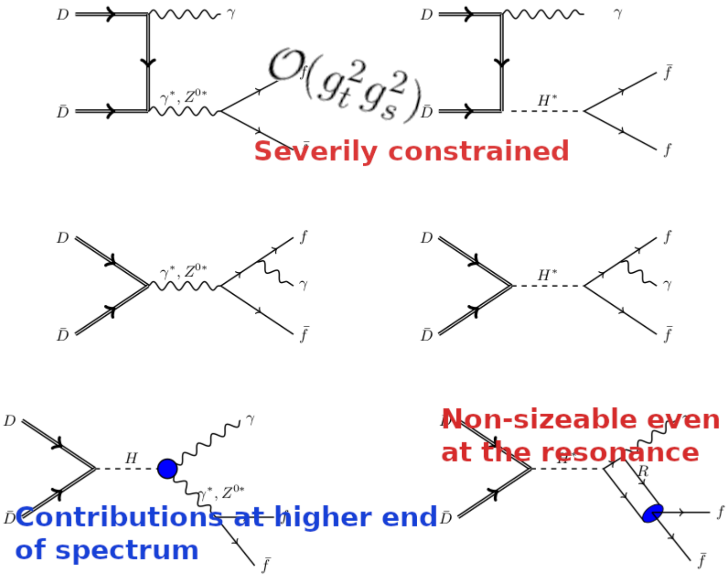

⟵ Initial state radiation.

⟵ Final state radiation.

⟵ Internal radiation.

Contributions to Prompt Photon Flux

Prompt photon production in FSR:

- Direct emission
- Decay products (leptons)
- Particle jets from hadronization of quarks

The last two modify our results for all fermions except for e and μ, which do not have hadronic decays and are only affected by suppressed higher order EW radiative corrections.

We employ the packages of DarkSusy and PPC4DMID to calculate these fluxes, including radiative corrections.

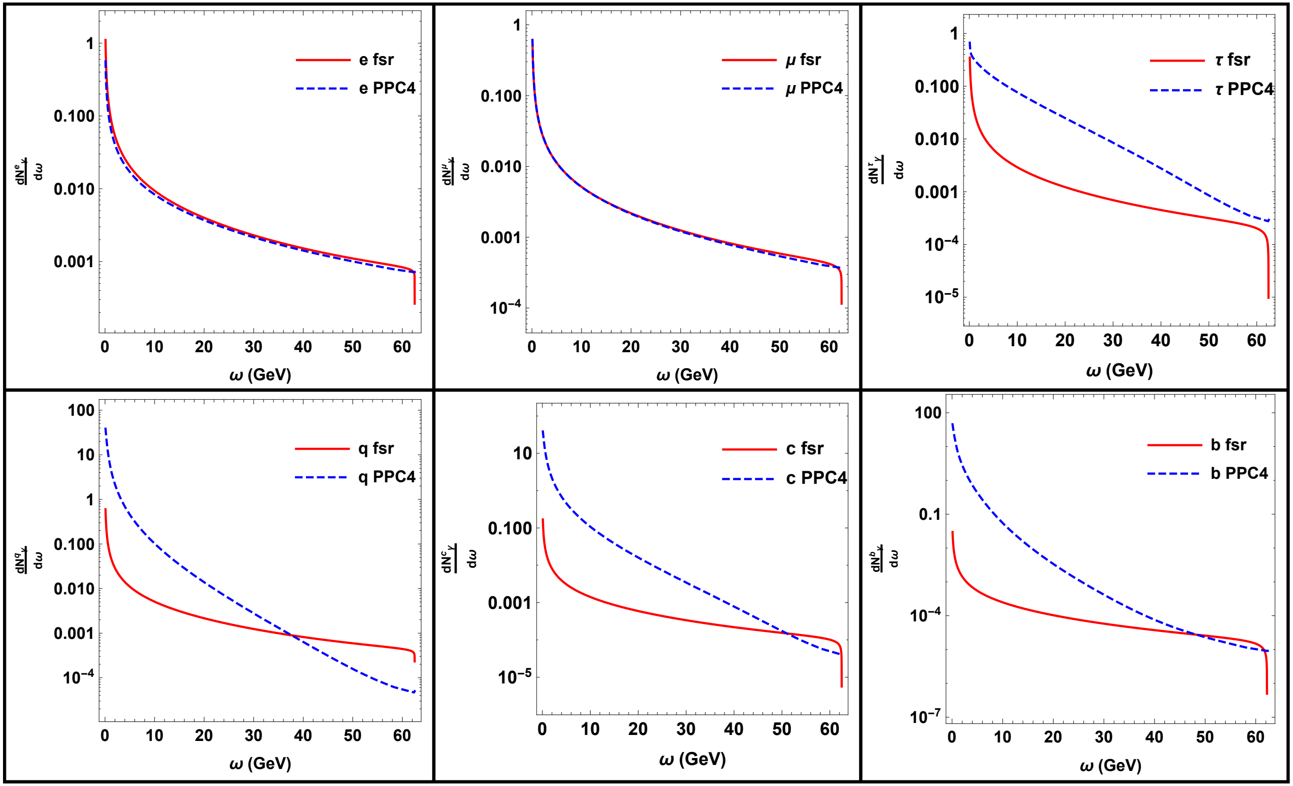

Comparison of the direct photon emission versus the spectrum from PPC4DMID for M=62.5 GeV.

Prompt Photon Flux from SODM

The prompt photon flux contributions for $g_s = 10^{-3}$ and M=62.49 GeV. We use the gNFW profile with $\gamma = 1.25$, within a ROI with $|l| < 10^\circ$ and $2^\circ < |b| < 10^\circ$, which yields a J-factor $J_0 = 7.12 \times 10^5$ GeV$^4/cm^2$ seg.

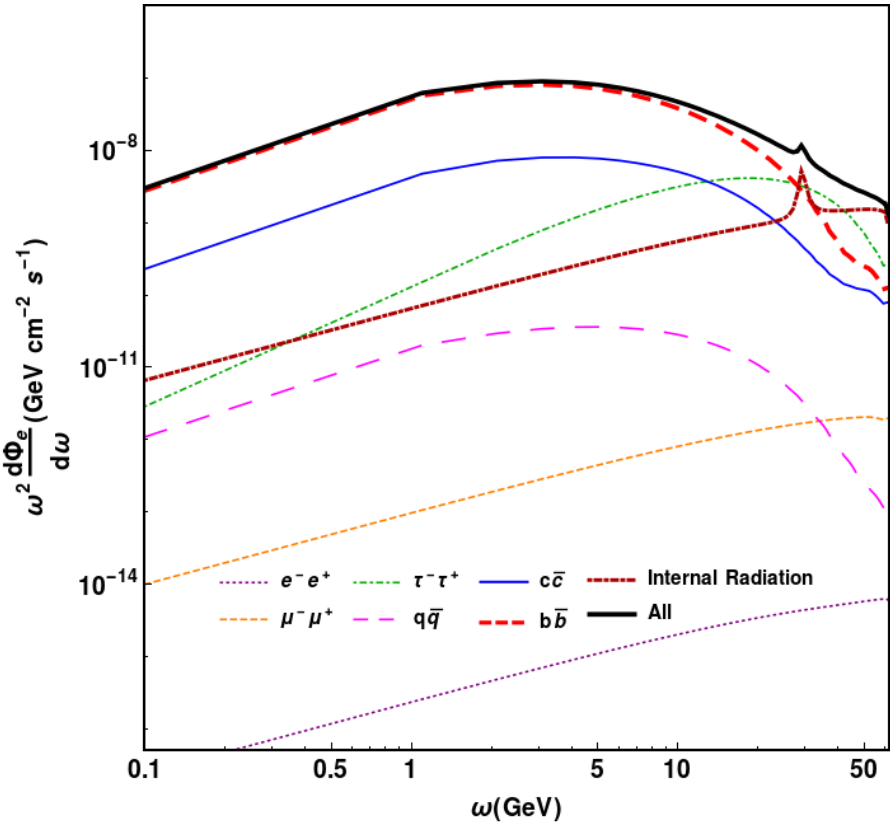

Delayed emission: Inverse Compton Scattering (ICS)

Delayed photon emission by ICS can be produced in at least three instances:

- Propagation of electrons produced in $\bar{D}D \to e^+e^-$.
- Propagation of electrons produced in decays of leptons or hadronization of quarks from $\bar{D}D \to \bar{f}f$.
- Propagation of muons produced in $\bar{D}D \to \mu^+\mu^-$.

These contributions were calculated with the NFW density profile since the PPC4DMID tabulated spectrum is designed for a number of profiles that don't include the gNFW. However, the contributions are not sensitive to the choice of density profile, so the results are compatible.

Delayed emission: Inverse Compton Scattering (ICS)

Delayed photon emission by ICS can be produced in at least three instances:

- Propagation of electrons produced in $\bar{D}D \to e^+e^-$. $\longrightarrow$ Negligible due to small couplings.
- Propagation of electrons produced in decays of leptons or hadronization of quarks from $\bar{D}D \to \bar{f}f$.
- Propagation of muons produced in $\bar{D}D \to \mu^+\mu^-$. $\longrightarrow$ Three orders of magnitude below thermal cross section for this mass window.

These contributions were calculated with the NFW density profile since the PPC4DMID tabulated spectrum is designed for a number of profiles that don't include the gNFW. However, the contributions are not sensitive to the choice of density profile, so the results are compatible.

ICS Flux from SODM

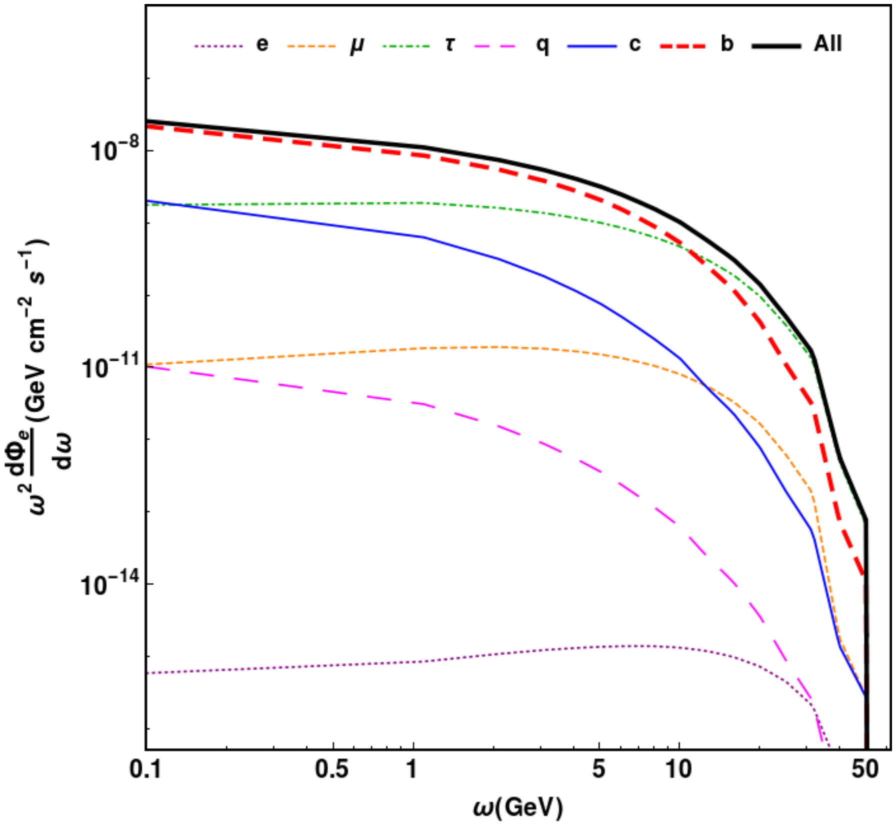

Contributions to the differential photon flux from ICS.

GRE Contributions: Final Results

Considering the uncertainty band for the GRE obtained by FermiLAT, the values of $g_s \in [0.98, 1.01] \times 10^{-3}$ and $M \in [62.470, 62.505]$ GeV are consistent with the excess data.

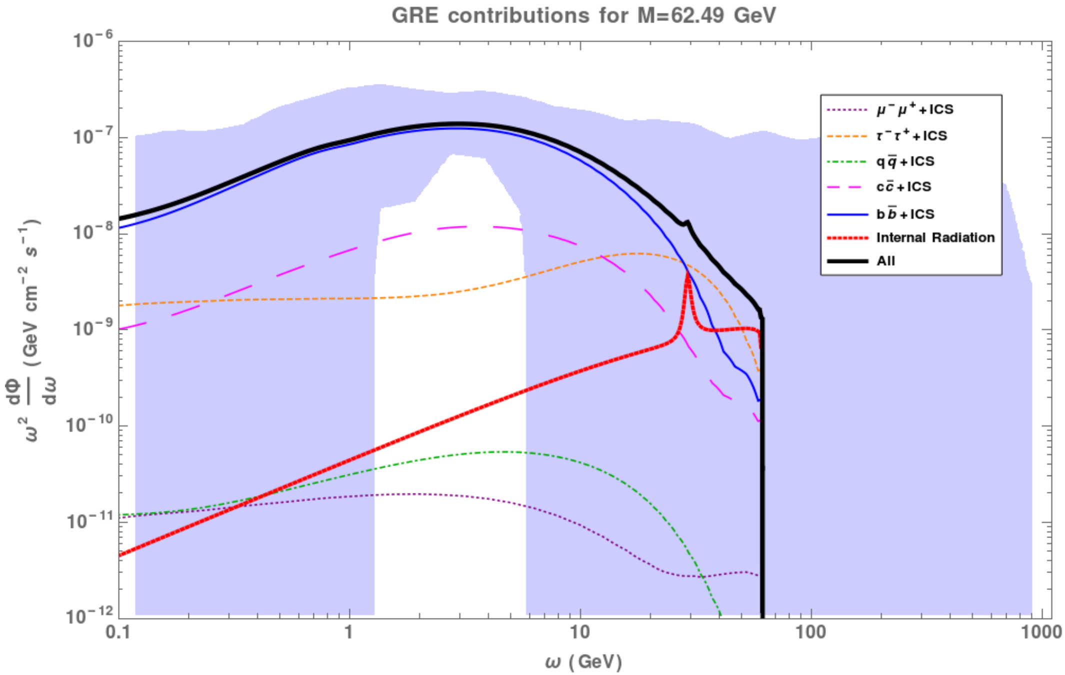

Differential flux including all the contributions, for M=62.49 GeV and $g_s = 9.81 \times 10^{-4}$.

Thermal average cross-section

- We are at the resonance. Resonant effects break down the non-relativistic calculation of DM relic density.
- Must calculate it using the complete $\langle \sigma v_r \rangle (x)$

Expansion (dashed line):

$$\langle \sigma v_r \rangle \simeq a + b/x$$

Complete (solid line):

$$\langle \sigma v_r \rangle = \frac{\int \sigma v_r e^{-E_1/T} e^{-E_2/T} d^3p_1 d^3p_2}{\int e^{-E_1/T} e^{-E_2/T} d^3p_1 d^3p_2}$$

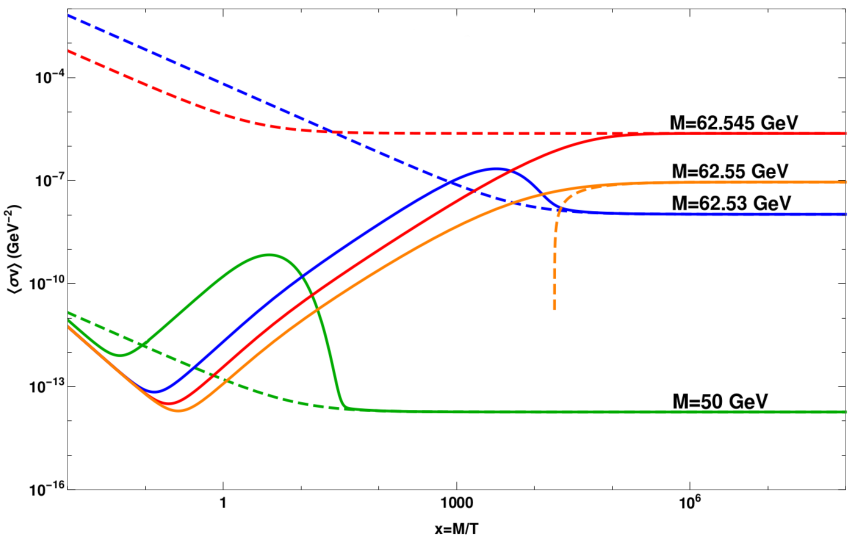

g_s consistent with Relic Density and Xenon1T

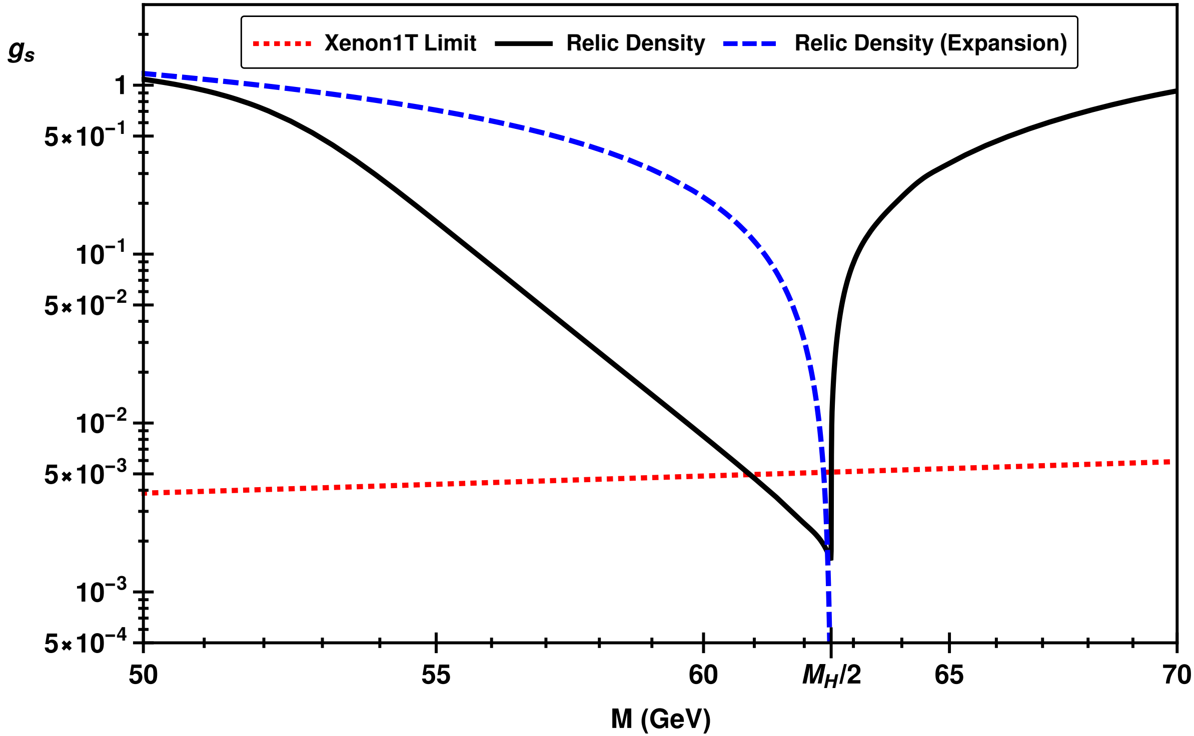

Bounds to $\bar{D}D \to \mu^+\mu^-, \tau^+\tau^-$

⊛ Upper limit for the μ channel: $\langle \sigma v_r \rangle_{\mu^+\mu^-} \leq 8.96 \times 10^{-26} cm^3/seg$ for $M \cong 62.5$ Gev.

L. Bergstrom, T. Bringmann, I. Cholis, D. Hooper and C. Weniger, Phys. Rev. Lett. 111 171101 (2013). arXiv: 1306.3983

For SODM: Largest value in the GRE-consistent mass region: $\langle \sigma v_r \rangle_{\mu^+\mu^-} = 8.30 \times 10^{-30} cm^3/seg$ for $M \cong 62.505$ Gev and $g_s = 9.81 \times 10^{-4}$.

⊛ Upper limit for the τ channel: $\langle \sigma v_r \rangle_{\mu^+\mu^-} \leq 1.2 \times 10^{-26} cm^3/seg$ for $M \cong 62.5$ Gev.

DES, Fermi-LAT collaboration, Astrophys. J. 809 L4 (2015). arXiv: 1503.02632

For SODM: Largest value in the GRE-consistent mass region: $\langle \sigma v_r \rangle_{\mu^+\mu^-} = 2.42 \times 10^{-27} cm^3/seg$ for $M \cong 62.505$ Gev and $g_s = 9.81 \times 10^{-4}$.

Other constraints: $\bar{b}b$ limits

Indirect detection: Obtained from a combined analysis of the energy flux from 45 dwarf spheroidal galaxies (dSph).

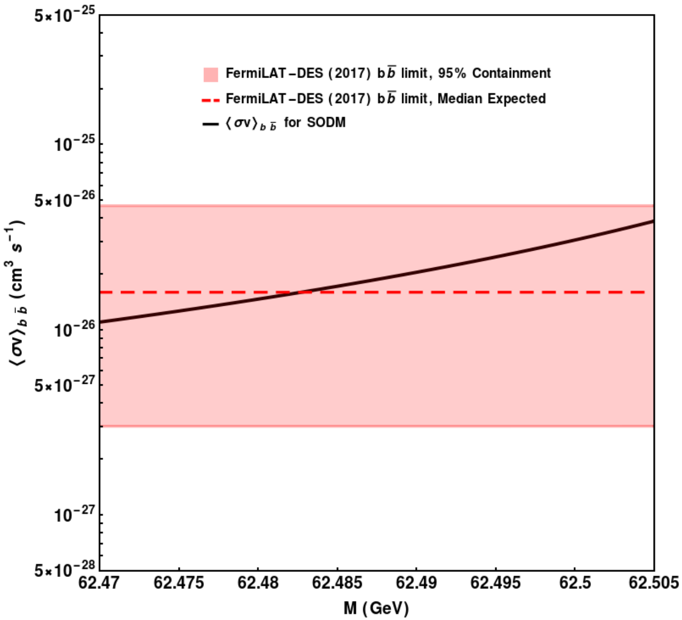

DES, Fermi-LAT collaboration, Astrophys. J. 809 L4 (2015). arXiv: 1503.02632.

Other constraints: $\bar{b}b$ limits

Indirect detection: Obtained from a combined analysis of the energy flux from 45 dwarf spheroidal galaxies (dSph). $\longrightarrow$ Only 19 targets have a J-factor derived from experimental data on stellar dynamics (Astrophys. J. 801 (2015) 74. arXiv: 1408.0002.)

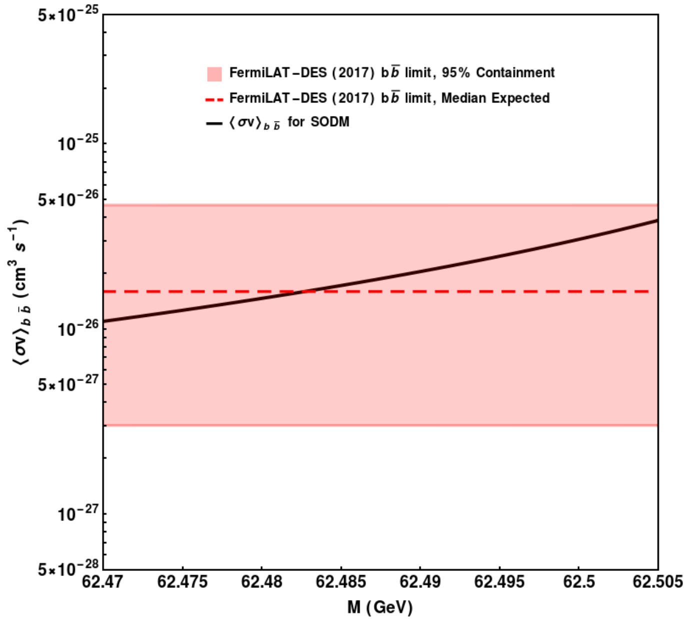

DES, Fermi-LAT collaboration, Astrophys. J. 809 L4 (2015). arXiv: 1503.02632.

Other constraints: Indirect detection in dSph galaxies

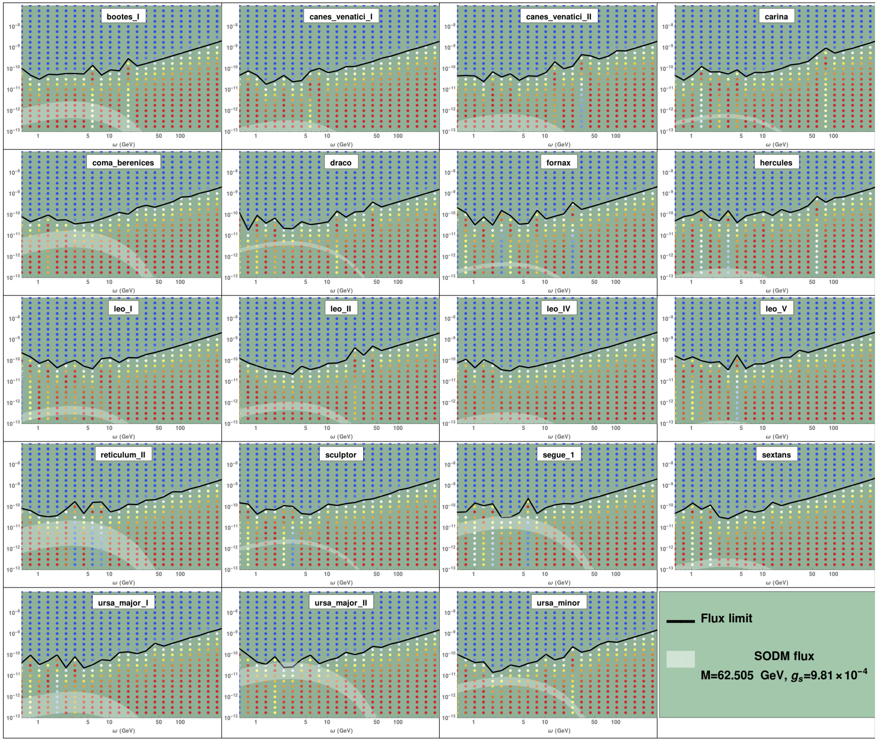

Bin-by-bin upper bound for the photon flux for the 19 targets, using the likelihood function data from *Astrophys. J. 834 (2017) 110. arXiv: 1611.03184*.

Other constraints: $\gamma\gamma$ limits

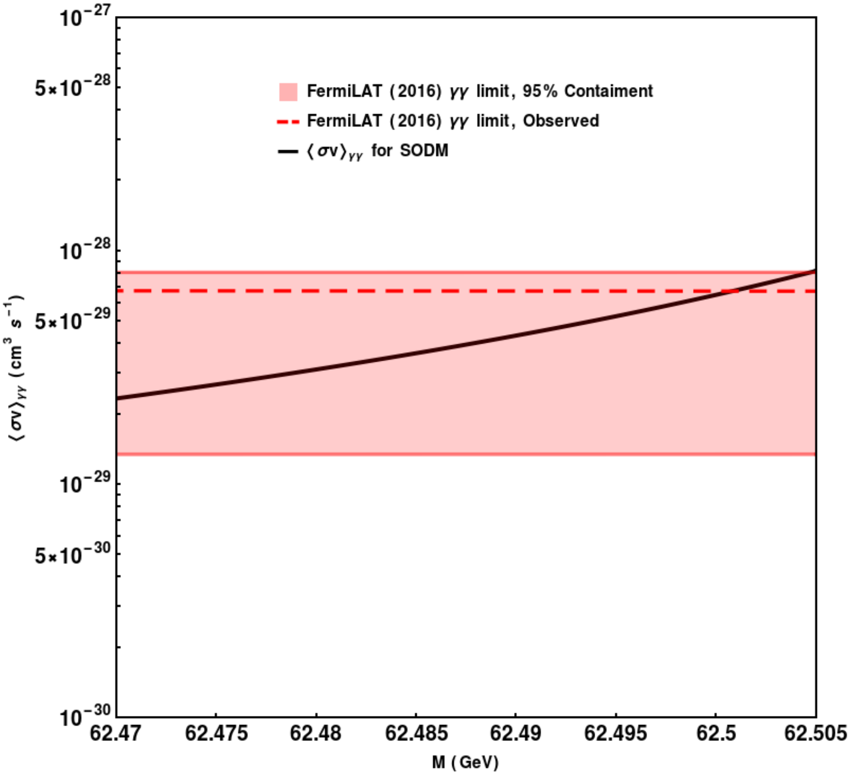

Fermi-LAT collaboration, Phys. Rev. D91 (2015) 122002. arXiv: 1506.00013.

Conclusions

- Taking into account all the contributions we found a good agreement with the GRE data for the windows $g_s \in [0.98, 1.01] \times 10^{-3}$ and $M \in [62.470, 62.505]$ GeV.
- This results are in agreement with constrains from relic density, when using the full (relativistic) annihilation cross sections, finding substantial modifications near the resonance.
- The results are also consistent with XENON1T limits for direct detection and constraints for annihilation cross sections of $\mu^+\mu^-$, $\tau^+\tau^-$ and $\gamma\gamma$.
- For these values of M and g_s, annihilation into $\bar{b}b$ is in agreement with the energy flux limit from the 45 dSph galaxies, and we also performed a detailed bin-by-bin analysis for the 19 targets with a measured J-factor.
- Lowering the $\bar{b}b$ and $\gamma\gamma$ upper bounds would give definite tests of the possibility that DM has a $(1,0) \oplus (0,1)$ space-time structure and a mass $M \approx M_H/2$.

THANK YOU!

See full work:
JHEP **08**, 106 (2020), doi:10.1007/JHEP08(2020)106
[arXiv:1911.01604 [hep-ph]].

Invisible Width and Relic Density